# Chapter 2
Brain Sensors and Signals

2.1 Relevant Sensors

A variety of sensors for monitoring brain activity exist, and could in principle provide the basis for a BCI. These include, besides electroencephalography (EEG) and more invasive electrophysiological methods such as electrocorticography (ECoG) and recordings from individual neurons within the brain, magnetoencephalography (MEG), positron emission tomography (PET), functional magnetic resonance imaging (fMRI), and optical imaging (i.e., functional Near InfraRed (fNIR)). However, MEG, PET, fMRI, and fNIR are still technically demanding and expensive, which impedes widespread use. Despite these impediments, several studies have recently explored the value of these modalities for BCI research [10, 11, 42, 60, 82, 97, 98, 108–110, 118]. Furthermore, PET, fMRI, and fNIR, which depend on metabolic processes, have long time constants and thus seem to be less amenable to rapid communication. At present, non-invasive and invasive electrophysiological methods (i.e., EEG, ECoG, and single-neuron recordings, see illustration in Fig. 2.1) are the only methods that use relatively simple and inexpensive equipment and have high temporal resolution. Thus, these three alternatives are at present the only methods that can offer the possibility of a new non-muscular communication and control channel – a practical brain–computer interface.

The first and least invasive alternative uses EEG, which is recorded from the scalp [6, 22, 39, 40, 54, 59, 61, 64, 73, 76, 101, 106, 114, 116, 117]. These BCIs support much higher performance than previously assumed, including two- and three-dimensional cursor movement [59, 66, 114]. However, the acquisition of such high levels of control typically requires extensive user training. Furthermore, EEG has low spatial resolution, which will eventually limit the amount of information that can be extracted, and it is also susceptible to artifacts from other sources.

The second alternative uses ECoG, which is recorded from the cortical surface [23, 46, 47, 111]. It has higher spatial resolution than EEG (i.e., tenths of millimeters vs. centimeters [25]), broader bandwidth (i.e., 0–500 Hz [99] vs. 0–50 Hz), higher characteristic amplitude (i.e., 50–100 µV vs. 10–20 µV), and far less vulnerability to artifacts such as EMG [3, 25] or ambient noise. While this method is invasive,

Fig. 2.1 Different types of sensors most commonly used in BCI research. *A*: Electrodes are placed non-invasively on the scalp (electroencephalography (EEG)). *B*: Electrodes are placed on the surface of the brain (electrocorticography (ECoG)). *C*: Electrodes are placed invasively within the brain (single-neuron recordings). (From [112])
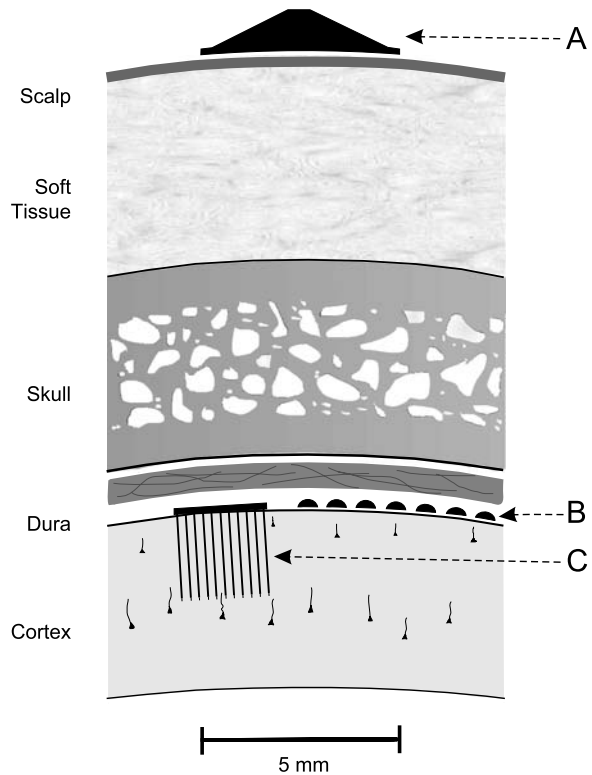
the use of these electrodes that do not penetrate the cortex may combine excellent signal fidelity with good long-term stability [7, 49, 52, 119].

The third and most invasive alternative uses microelectrodes to measure local activity (i.e., action or field potentials) from multiple neurons within the brain [21, 32, 45, 67, 84, 92, 95, 103]. Signals recorded within cortex have higher fidelity and might support BCI systems that require less training than EEG-based systems. However, clinical implementations of intracortical BCIs are currently impeded mainly by the difficulties in maintaining stable long-term recordings [20, 93, 100], by the substantial technical requirements of single-neuron recordings, and by the need for continued intensive expert oversight. For these reasons, practically all BCI demonstrations in humans to date have been achieved with, and the examples in this book are using or meant for, EEG or ECoG recordings.

2.2 Brain Signals and Features

2.2.1 Using Brain Signals for Communication

Successful creation of a new communication channel – directly from the brain to an output device – depends on two requirements. The first requirement is the use of an

adequate sensor that can effectively measure the brain signal features that can communicate a user's intent. As described in the previous section, multiple sensors exist that can in principle detect relevant signals. Practicality and speed considerations exclude most of these options, so that almost all BCI systems to date depend on detection of electrophysiological signals using sensors on the scalp, on the surface of the brain, or within the brain. In humans, safety and/or stability issues have confined most studies to electroencephalographic (EEG) recordings from the scalp. The second requirement is the definition and negotiation of a mutual language (i.e., brain signal features such as time-domain or frequency-domain measurements at particular locations), so that, as in any other communication system, the user may use the symbols of this language to communicate intent, and the computer can detect these symbols and effect this intent.

For two reasons, the language of BCI communication cannot be completely arbitrary. First, the brain might simply not be physically able to produce the symbols of this language. For example, one might define the arbitrary language as the amplitude coherence between two different frequency bands at one particular location, and its symbols could be discrete coherence amplitudes, but the brain might simply not be physically able to produce changes in coherence amplitude at the selected frequencies and locations. Second, the brain might be able to produce the symbols of this language, but might not be able to use them to convey intent. For example, one might define the arbitrary language as amplitude modulations at 10 Hz over visual areas of the brain. Many studies have shown that repetitive visual stimuli at particular frequencies (such as 10 Hz) can evoke oscillatory responses in the brain [63], so clearly the brain is physically able to modulate activity at 10 Hz and can thus produce different symbols of that arbitrary language. However, it might not be able to produce these symbols without the visual stimuli, or might not be able to use these symbols to convey intent.

In summary, there is no theoretical basis for selecting the language (i.e., brain signal) that is most useful for BCI communication. Furthermore, any clinically successful BCI will necessarily be under the influence of practical considerations such as risk, benefit, and price. Thus, it is currently unclear which brain signal and which sensor modality (EEG, ECoG, or single neuron recordings) will ultimately be most beneficial given these constraints. At the same time, experimental evidence is able to provide some guidance on which brain signals to utilize for BCI communication. For example, many studies have shown that particular imagined tasks (e.g., hand movements) have detectable effects on particular brain signals. Taking advantage of this phenomenon, people can communicate simple messages using imagery of hand movements. Other studies have shown that the presentation of desired stimuli produces detectable brain signal responses. By presenting multiple stimuli and by detecting the response to the desired stimulus, people can communicate which item they desire. These two possibilities are representative for the phenomena most relevant for BCI communication in humans, and are described in more detail in the following two sections.
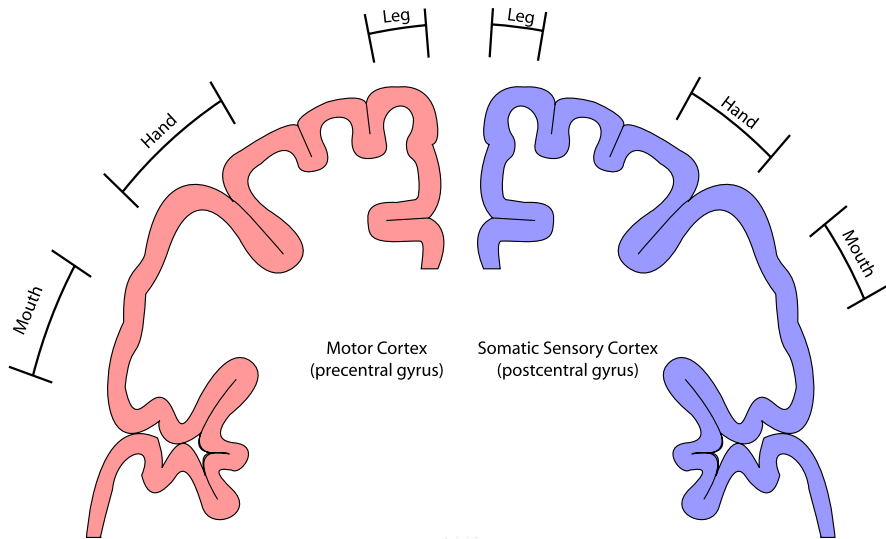
Fig. 2.2 The brain figure on the top shows a vertical cross-section along motor (*left*) and sensory (*right*) cortical areas. The motor cortex is displayed in *red*. Particular areas in the motor cortex are associated with function of particular limbs (i.e., "motor homunculus"). Similarly, sensory cortex is shown in *blue*. Particular areas in sensory cortex are also associated with sensory function of different limbs (i.e., "sensory homunculus")

2.2.2 Mu/Beta Oscillations and Gamma Activity

Most people exhibit prominent oscillations in the 8–12 Hz band of the EEG recorded over sensorimotor areas (see Fig. 2.2) when they are not actively engaged in motor action, sensory processing, or in imaginations of such actions or processing [24, 27, 37] (reviewed in [69]). This oscillation is usually called mu rhythm and is thought to be produced by thalamocortical circuits [69]. The lack of modern acquisition and processing methodologies have initially not made it possible to detect the mu rhythm in many people [8], but computer-based analyses have since revealed that the mu rhythm is in fact present in a large majority of people [70, 71]. Such analyses have also demonstrated that the mu rhythm is usually associated with 18–25 Hz beta rhythms. While some of these beta rhythms are harmonics of mu rhythms, some are separable by topography and/or timing from mu rhythms, and thus at least appear to be independent EEG features [57, 70, 71].

Because mu/beta rhythm changes are associated with normal motor/sensory function, they could be good signal features for BCI-based communication. Movement or preparation for movement, but typically not specific aspects of movements such as its direction [104], are typically accompanied by a decrease in mu and beta activity over sensorimotor cortex, particularly contralateral to the movement. Furthermore, mu/beta rhythm changes also occur with motor imagery (i.e., imagined movement) [57, 72]. Because people can change these rhythms without engaging
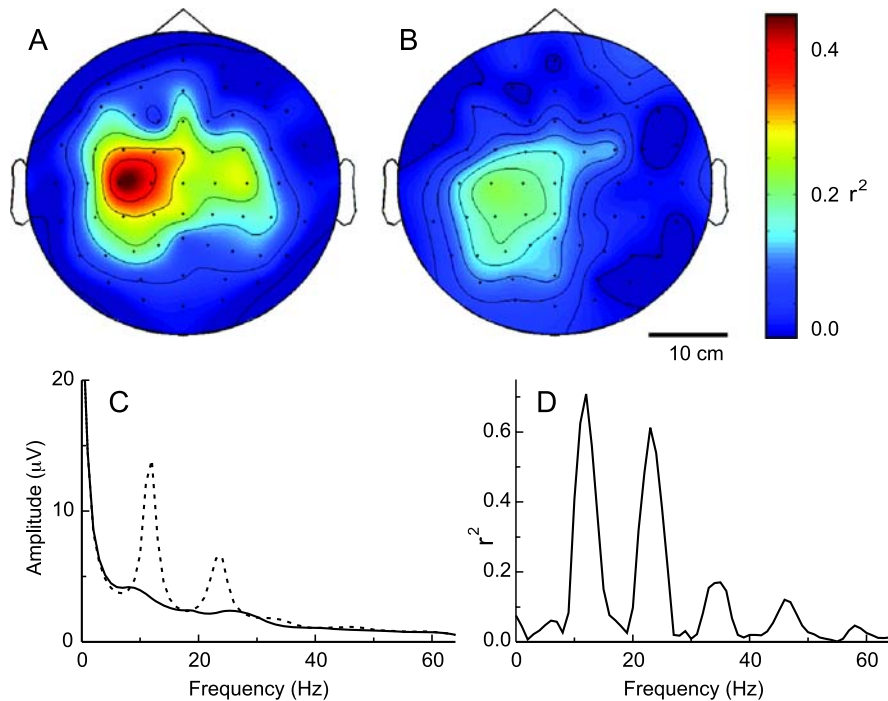
Fig. 2.3 Examples of mu/beta rhythm signals (modified from [85]). **A**, **B**: Topographical distribution on the scalp of the difference (measured as r^2 (the proportion of the single-trial variance that is due to the task)), calculated for actual (**A**) and imagined (**B**) right-hand movements and rest for a 3-Hz band centered at 12 Hz. **C**: Example voltage spectra for a different subject and a location over left sensorimotor cortex (i.e., C3 (see [94])) for comparing rest (*dashed line*) and imagery (*solid line*). **D**: Corresponding r^2 spectrum for rest vs. imagery. Signal modulation is focused over sensorimotor cortex and in the mu- and beta-rhythm frequency bands

in actual movements, these rhythms could serve as the basis for a BCI. Figure 2.3 shows the basic phenomenon of mu/beta-rhythm modulations in the EEG.

Similar to EEG, activity in the mu/beta bands recorded using ECoG also decreases with motor tasks [12, 14, 28, 48, 62, 77, 96]. In addition, activity in the gamma range (i.e., >40 Hz) has been found to increase with these tasks [13, 47, 48, 62]. With isolated exceptions (e.g., [74]), task-related changes in these higher frequencies have not been reported in the EEG. There are indications that gamma activity reflects activity of local neuronal groups [41, 62], and thus could be most directly reflective of specific details of movement. Indeed, recent studies have shown relationships of gamma activity with specific kinematic parameters of hand movements [9, 79, 83, 86].

In summary, many studies have shown using EEG [36, 54, 61, 64, 73, 113–116] or ECoG [23, 46, 47, 87, 111] that humans can use motor imagery to modulate activity in the mu, beta, or gamma bands, and to thereby control a BCI system.
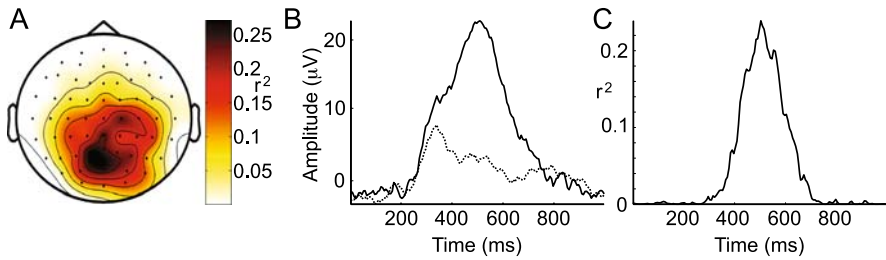
Fig. 2.4 Example characteristics of the P300 response (data courtesy of Dr. Eric Sellers, Wadsworth Center/East Tennessee State University). *Left*: Topographical distribution of the P300 potential at 500 ms after stimuli, measured as r^2 and calculated between desired and not desired stimuli. *Center*: The time courses at electrode location Pz of the voltages for desired (*solid line*) or not desired (*dashed line*) stimuli. *Right*: Corresponding r^2 time course

2.2.3 The P300 Evoked Potential

In addition to brain responses modulated by motor action or motor imagery, evoked potentials may also be useful for BCI operation. For example, numerous studies over the past four decades have shown that presentation of infrequent stimuli typically evokes a positive response (called the "P300" or "oddball" potential) in the EEG over parietal cortex about 300 ms after stimulus presentation (see [17, 102, 107]; [15, 18, 80] for review; Fig. 2.4). The amplitude of the P300 potential is largest at the parietal electrode sites and is attenuated as the recording sites move to central and frontal locations [15]. A P300 is usually elicited if four conditions are met. First, a random sequence of stimulus events must be presented. Second, a classification rule that separates the series of events into two categories must be applied. Third, the user's task must require using the rule. Fourth, one category of events must be presented infrequently [16].

Using experimental paradigms that implement these four conditions, the P300 potential has been used as the basis for a BCI system in many studies [1, 5, 19, 22, 33, 68, 78, 88–91, 106]. The classical format developed by Donchin and colleagues [22] presents the user with a matrix of characters (Fig. 2.5). The rows and columns in this matrix flash successively and randomly at a rapid rate (e.g., eight flashes per second). The user selects a character by focusing attention on it and counting

Fig. 2.5 The classical P300-based spelling paradigm developed by Donchin [19, 22]. Rows and columns of the matrix flash in a block-randomized fashion. The row or column that contains the desired character evokes a P300 potential

how many times it flashes. The row or column that contains this character evokes a P300 response, whereas all others do not. After averaging several responses, the computer can determine the desired row and column (i.e., the row/column with the highest P300 amplitude), and thus the desired character.

2.3 Recording EEG

2.3.1 Introduction

After discussing the brain signals most commonly used for BCI operation, this section describes the relevant principles of brain signal recordings and the types of signal artifacts that are typically encountered. These descriptions are mostly focused on EEG. The same general recording principles also apply to ECoG recordings. While most types of artifacts are typically encountered only with EEG, artifacts can also be detected in ECoG [3]. Brain signals are detected using different types of metal electrodes that are placed on the scalp (EEG) or on the surface of the brain (ECoG). These electrodes measure small electrical potentials that reflect the activity of neurons within the brain. To detect the tiny amplitude of these signals, they first have to be amplified. Any biosignal amplifier measures the potential difference (i.e., the voltage) between two electrodes. In most BCI systems, the second of these two electrodes is always the same, i.e., measurements are "unipolar" rather than "bipolar." In other words, measurements from all electrodes are referred to one common electrode, which consequently is called "reference," and typically labeled *Ref*. To improve signal quality, amplifiers require the connection of a "ground" electrode, which is typically labeled *Gnd*.

EEG electrodes are small metal plates that are attached to the scalp using a conducting electrode gel. They can be made from various materials. Most frequently, tin electrodes are used, but there are gold, platinum, and silver/silver-chloride (Ag/AgCl) electrodes as well. Tin electrodes are relatively inexpensive and work well for the typical BCI-related application. At the same time, tin electrodes introduce low-frequency drifting noise below 1 Hz, which makes them unsuitable for some applications (e.g., Slow Cortical Potential measurements or low-noise evoked potential recordings).

An important but often neglected detail: mixing electrodes made from different materials in the same recording will result in DC voltage offsets between electrodes. These offsets are due to electrochemical contact potentials and can often be larger in amplitude than what a typical amplifier can tolerate. This will result in a greatly diminished signal-to-noise ratio. Thus, you should always use electrodes made from the same material in a particular recording.

2.3.2 Electrode Naming and Positioning

The standard naming and positioning scheme for EEG applications is called the 10–20 international system [35]. It is based on an iterative subdivision of arcs on

the scalp starting from particular reference points on the skull: Nasion (Ns), Inion (In), and Left and Right Pre-Auricular points (PAL and PAR, respectively). The intersection of the longitudinal (Ns–In) and lateral (PAL–PAR) diagonals is named the Vertex, see Fig. 2.6-A. The 10–20 system originally included only 19 electrodes (Fig. 2.6-B, [35]). This standard was subsequently extended to more than 70 electrodes (Fig. 2.6-C, [94]). This extension also renamed electrodes T3, T5, T4, and T6, into T7, P7, T8, and P8, respectively. Sometimes, one of the electrodes mounted in these positions is used as reference electrode. More often, the ear lobe or mastoid (i.e., bony outgrowth behind the ear) are used. For example, a typical recording may have the ground electrode placed on the mastoid and the reference on the ear lobe on the opposite side.

Acquiring EEG from more than a single location is necessary to be able to determine the optimum location for the BCI purpose. It also greatly facilitates the identification of signal artifacts. Thus, for research purposes we strongly recommend to record from as many locations as possible – at least from 16. For clinical applications, we suggest to initially record from at least 16 locations. Once effective BCI operation has been established and the optimal locations have been determined, the electrode montage can be optimized to record from fewer locations.

2.3.3 Important Brain Areas and Landmarks for BCIs

The brain consists of several distinct areas and landmarks. The approximate location of these areas and landmarks can be determined from the extended 10–20 system shown in Fig. 2.6-C. One of these landmarks is the central sulcus, which is also called Rolandic fissure. The central sulcus runs approximately along the lines between electrodes CPz–C2–C4 and CPz–C1–C3, respectively. On each hemisphere, the central sulcus divides the brain into the frontal lobe (in frontal direction, i.e., toward the nose) and parietal lobe (in posterior direction, i.e., toward the back of the head). The frontal lobe contains, among other areas, the primary motor cortex, i.e., the area of the brain that is most immediately involved in the execution of movements. The parietal lobe contains, among other areas, primary sensory cortex, i.e., the area of the brain that is a direct neighbor of the primary motor cortex and that is most directly involved in processing sensory information from different body parts. Another important landmark is the Sylvian fissure, which is also called lateral sulcus. It runs along the lines connecting CP6–C6–FT8–FT10 and CP5–C5–FT7–FT9, respectively. It separates the temporal lobe, an area in the brain responsible for auditory processing and memory, from the frontal and parietal lobes.

2.3.4 Placing Electrodes with a Cap

Accurate placement of many electrodes on the scalp is time consuming and requires practice. EEG caps greatly facilitate this process. These caps are made of elastic
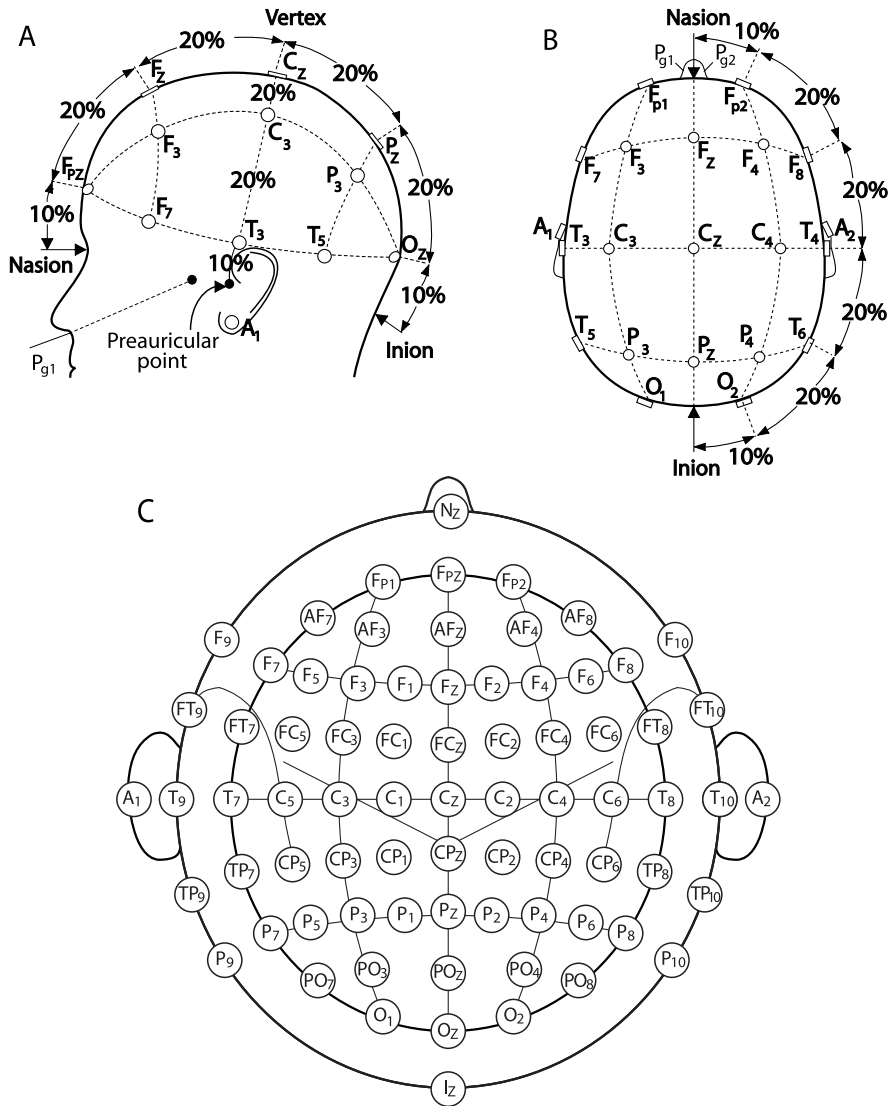
Fig. 2.6 Electrodes on the original 10–20 scheme (figures **A** and **B**, re-drawn from [35]). Current extensions to this scheme define more than 70 locations (figure **C**, re-drawn from [94])

fabric (often available in different sizes), and electrodes are already fixed in the proper configuration. One proven technique to place electrodes using such caps is the following:

- Mark the vertex on the subject's scalp using a felt-tip pen or some other similar method. Begin by locating the nasion and inion on the subject as indicated in panel A of Fig. 2.6. Using a tape measure, find the distance between these two

locations. The point half-way between the two points is the vertex. Make a mark at that point for later reference. (Other 10–20 points could be located in a similar manner.)

- Mark scalp positions for Fpz and Oz. The Fpz position is above the nasion 10% of the distance from the nasion to the inion. The Oz position is above the inion the same distance.
- Identify the Cz electrode on the EEG cap and place the cap to position the Cz electrode on the vertex.
- Keeping Cz fixed, slide the cap onto the head.
- While ensuring that Cz does not shift, adjust the cap such that the Fz–Cz–Pz line is on the midline; Fp1–Fp2 line is horizontal, and at the level of the Fpz mark; the O1–O2 line is horizontal, and at the level of the Oz mark.
- You can now fix *Ref* and *Gnd* electrodes. These electrodes are attached in one of a few typical configurations. One common configuration is to attach the Ref electrode to one earlobe, and the Gnd electrode to the mastoid on the same side of the head. Another possible configuration is to attach Ref to one mastoid and Gnd to the other mastoid. This choice is influenced by the used cap technology, which may have separate electrodes outside the cap for reference and ground, or may have these electrodes embedded in the cap directly.

2.3.5 Removing Artifacts and Noise Sources

2.3.5.1 Introduction

Electrical power lines use sinusoidal voltages with a frequency of 50 or 60 Hz, depending on your country. Generally, 50 Hz are used in Europe, Asia, Africa, and parts of South America; 60 Hz are used in North America, and parts of South America. Voltages are typically 110 or 230 volts, and thus exceed the EEG's 50 to 100 microvolts by a factor of 2×10^6, or 126 dB. Therefore, mains interference is ubiquitous in EEG recordings, especially if taken outside specially equipped, shielded rooms. Most EEG amplifiers provide a so-called notch filter that suppresses signals in a narrow band around the power line frequency.

Amplifier notch filters are designed to suppress a certain amount of mains interference. When there is mains interference still visible in the signal after activating the amplifier's notch filter, this is often due to high electrode impedance (Fig. 2.7).

### 2.3.5.2 Artifacts due to Eye Blinks

Eye blink artifacts are generated by fast movements of the eyelid along the cornea, such as during an eye blink. By friction between lid and cornea, this movement results in charge separation, with a dominantly dipolar charge distribution, and the
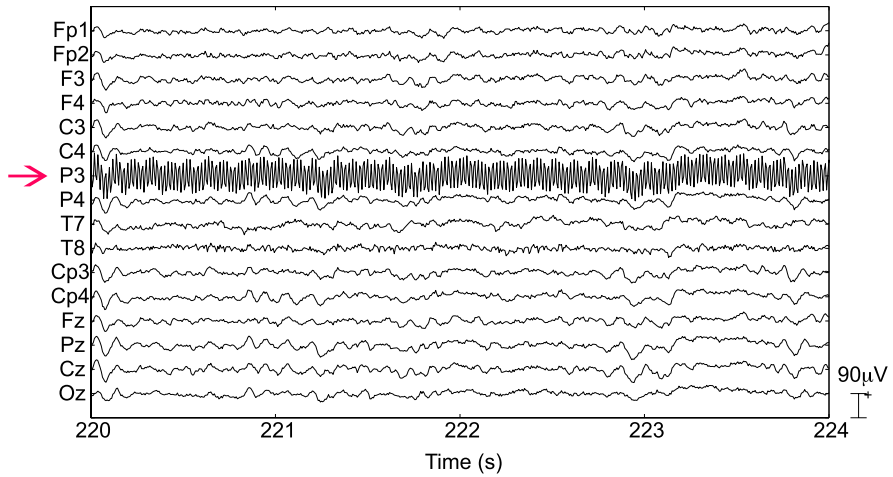
Fig. 2.7 Artifacts due to power line interference. This figure shows an example for one signal channel (marked by the *arrow*) that is contaminated by regular high frequency (i.e., 60 Hz) noise

dipole moment pointing in up-down-direction. In the EEG, this effect is recorded as a positive peak that lasts a few tenths of a second, is most prominent in the frontopolar region, but propagates to all the electrodes of the montage, attenuating with distance from the front (Fig. 2.8).

The frequency content of eye blink artifacts is negligible in the alpha band (around 10 Hz), so they have no strong effect on the use of sensorimotor rhythms. At the same time, their time-domain amplitude is quite large so that analyses in the
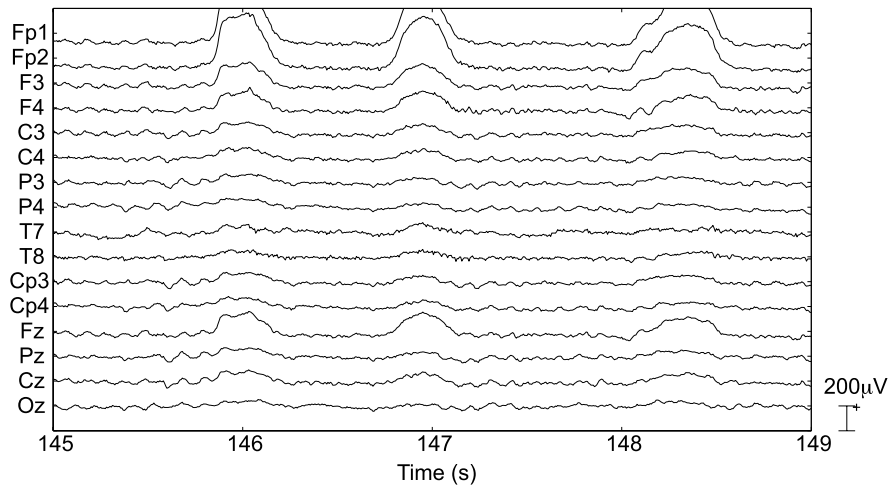
Fig. 2.8 Eye blink artifacts. This figure shows examples for signal contamination by eye blink artifacts. These artifacts are most prominent in frontal channels (channels *Fp1* and *Fp2*), but have effects on all channels
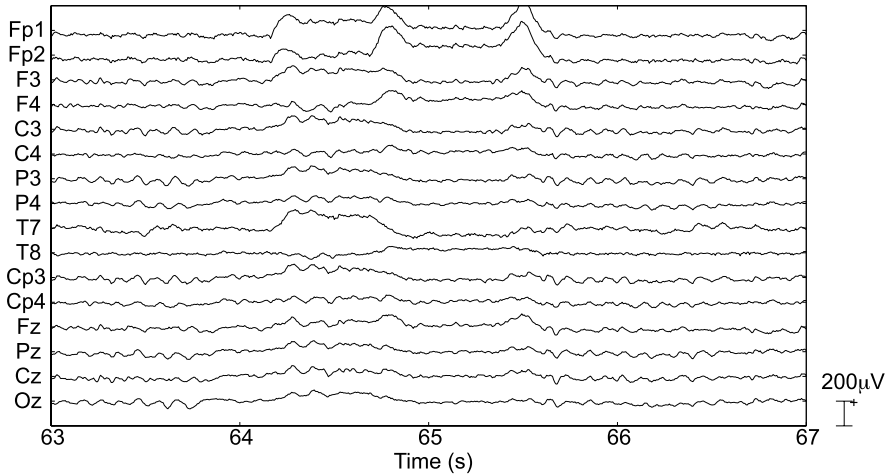
Fig. 2.9 Eye movement artifacts. Eye movements have a prominent effect on many channels. See the positive or negative deflections during early, middle and late parts of this recording

time domain (such as averaged P300 wave forms) can be strongly influenced by their presence.

2.3.5.3 Artifacts due to Eye Movements

Ocular artifacts (electrooculographic (EOG) signals) are produced by eye movements, and generated by a frictive mechanism that is similar to the one described above for eye blinks, except that it involves the retina and cornea rather than cornea alone. The effect on frontopolar and frontotemporal electrodes can be symmetric or asymmetric, depending whether the movement is vertical or horizontal, respectively. The effect of eye movement artifacts on frequency- or time-domain analysis is quite similar to that of blink artifacts, except that their frequency content is even lower, and amplitudes tend to be larger (Fig. 2.9).

2.3.5.4 Artifacts due to Muscle Movements

Muscular artifacts (electromyographic (EMG) signals, Fig. 2.10) must be carefully checked at the beginning of each recording, and verified throughout the recording. This is because the frequency distribution of EMG signals is very broad, so that they have a profound effect on amplitudes in typical mu/beta frequency ranges. The most common sources of EMG are the muscles that lift the eye brows, and those that close the jaw. Both groups of muscles can be inadvertently contracted during an experimental session. Keeping the mouth slightly open (or the tip of the tongue between the foreteeth) is a good strategy to avoid jaw-generated EMG.
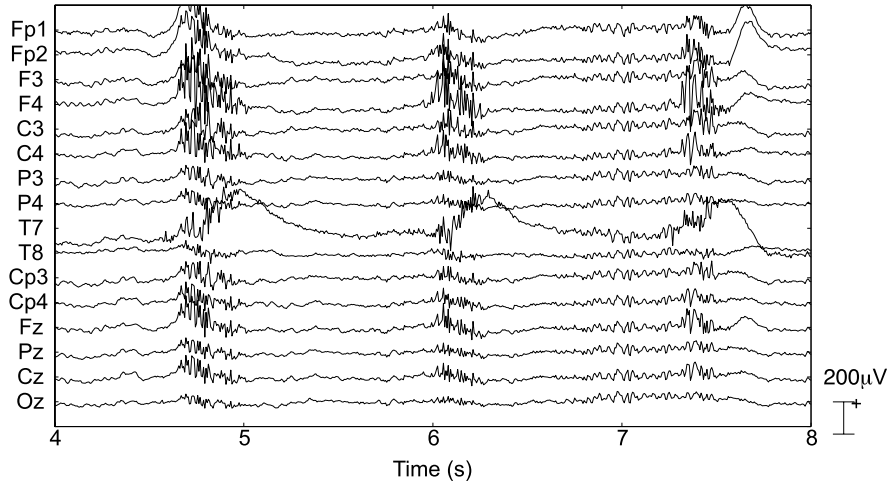
Fig. 2.10 Muscle movement artifacts. Many channels exhibit high frequency noise; in contrast to the power line interference, this noise is highly variable over time

2.4 BCI Signal Processing

The previous section described the two frequency- and time-domain phenomena most relevant to human BCI research, i.e., mu/beta rhythms and gamma activity, and the P300 evoked potential, respectively. Many studies have shown how these phenomena can be extracted and translated into device commands using different methods. All currently used procedures are listed in recent review articles on BCI feature extraction and translation methods [4, 50, 58]. The following sections describe an analysis approach that can realize many of these techniques. This approach is implemented in the example configurations of the BCI2000 software.

2.4.1 Introduction

BCI signal processing is a difficult problem. In addition to typical problems faced by any communication system (e.g., signals are contaminated with noise during transmission), it is initially and even during subsequent operation not clear which brain signals actually carry the message the user wants to communicate. In other words, it is the task of BCI signal processing to decode a message in a language we do not know much about. Fortunately, experimental evidence can provide some basic guidance. This guidance comes from observations that particular tasks (such as imagined hand movements) have particular effects on specific brain signals (such as the mu rhythm measured at a particular location). Even with this information, the choice of signals and tasks is still difficult, because it is likely that it is suboptimal (so that a completely different signal and task might provide improved performance) and
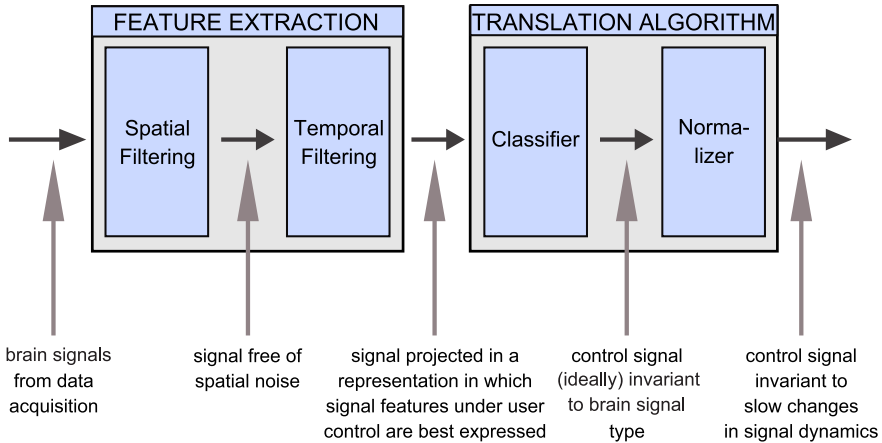
Fig. 2.11 Signal processing model utilized in BCI2000. This model consists of feature extraction and translation and can describe all common BCI methods

because it has to be optimized for each individual. In other words, even when only considering one possible physiological signal (such as the mu rhythm), the imagery task, best frequencies, and best locations have to be selected for each individual. The difficulty of choosing signals and tasks could be regarded as the *signal identification problem* of BCI communication. Assuming that a good candidate signal (e.g., the signal amplitude at a particular frequency or location) has been identified, traditional BCI signal processing usually employs two components to translate these signals into device commands: feature extraction and the translation algorithm.[1]

Feature extraction consists of two procedures: spatial filtering and temporal filtering (Fig. 2.11). Each of these procedures may have different realizations. The following paragraphs describe those realizations that are relevant to sensorimotor rhythm and P300 processing.

2.4.2 Spatial Filtering

The initial step in feature extraction is the application of a spatial filter that may have many possible realizations. The purpose of the spatial filter is to reduce the effect of spatial blurring. Spatial blurring occurs as an effect of the distance between the sensor and the signal sources in the brain, and because of the inhomogeneities of the tissues in between. Different approaches to spatial filtering have attempted

---

[1]We use the term *translation algorithm* instead of *classification* throughout this book, because the typically continuous nature of the device control signals produced by BCI signal processing is better expressed by the term translation algorithm rather than the discrete output that is typically implied by the term classification.

to reduce this blurring, and thus to increase signal fidelity. The most sophisticated approaches attempt to deblur signals using a realistic biophysical head model that is optimized for each user and whose parameters are derived from various sources such as magnetic resonance imaging (MRI) (e.g., [44]). While these approaches do increase signal quality in carefully controlled experiments, they are currently impractical for most experiments and for clinical applications. Other approaches do not require external parameterization of a complex model, but rather are simply driven by the signals that are submitted to it. For example, Independent Component Analysis (ICA) has been used to decompose brain signals into statistically independent components [51], which can be used to get a more effective signal representation. (This approach is called blind deconvolution in microscopy applications (e.g., [105]).) Even though these approaches have less demanding requirements than the more comprehensive modeling approaches, they require non-trivial calibration using sufficient amounts of data, and they produce output signals that will not necessarily correspond to actual physiological sources in the brain. Furthermore, while ICA optimizes statistical independence of brain signals, and can thus lead to more compact signal representations, it does not guarantee to optimize the discriminability of different brain signals in different tasks. Consequently, these complex model-based and data-driven approaches may not be amenable or desirable for typical BCI experimentation. A more appropriate technique is Common Spatial Patterns (CSP) [29, 81]. This technique creates a spatial filter (i.e., weights for the signals acquired at different locations) that correspond to their importance in discriminating between different signal classes. Finally, even simpler deblurring filters have been shown to be effective and yet practical [56]. These filters are essentially spatial high-pass filters with fixed filtering characteristics. Typical realizations include Laplacian spatial filters and the Common Average Reference (CAR) filter.

A Laplacian spatial filter is comprised of discretized approximations of the second spatial derivative of the two-dimensional Gaussian distribution on the scalp surface, and attempts to invert the process that blurred the brain signals detected on the scalp [31]. The approximations are further simplified such that, at each time point t, the weighted sum of the potential s_i of the four nearest or next nearest electrodes is subtracted from the potential s_h at a center electrode for the small and large Laplacian, respectively (see Eq. 2.1, Fig. 2.12(a), and Fig. 2.12(b)).

$$s_h'(t) = s_h(t) - \sum_{i \in S_i} w_{h,i} s_i(t) \tag{2.1}$$

In this equation, the weight $w_{h,i}$ is a function of the distance $d_{h,i}$ between the electrode of interest h and its neighbor i:

$$w_{h,i} = \frac{\frac{1}{d_{h,i}}}{\sum_{i \in S_i} \frac{1}{d_{h,i}}} \tag{2.2}$$

In practice, this filter is often implemented simply by subtracting the average of the four next nearest neighbors (i.e., the weight for each neighbor is -0.25) from the center location.

(a) Small Laplacian   (b) Large Laplacian   (c) Common average refer-
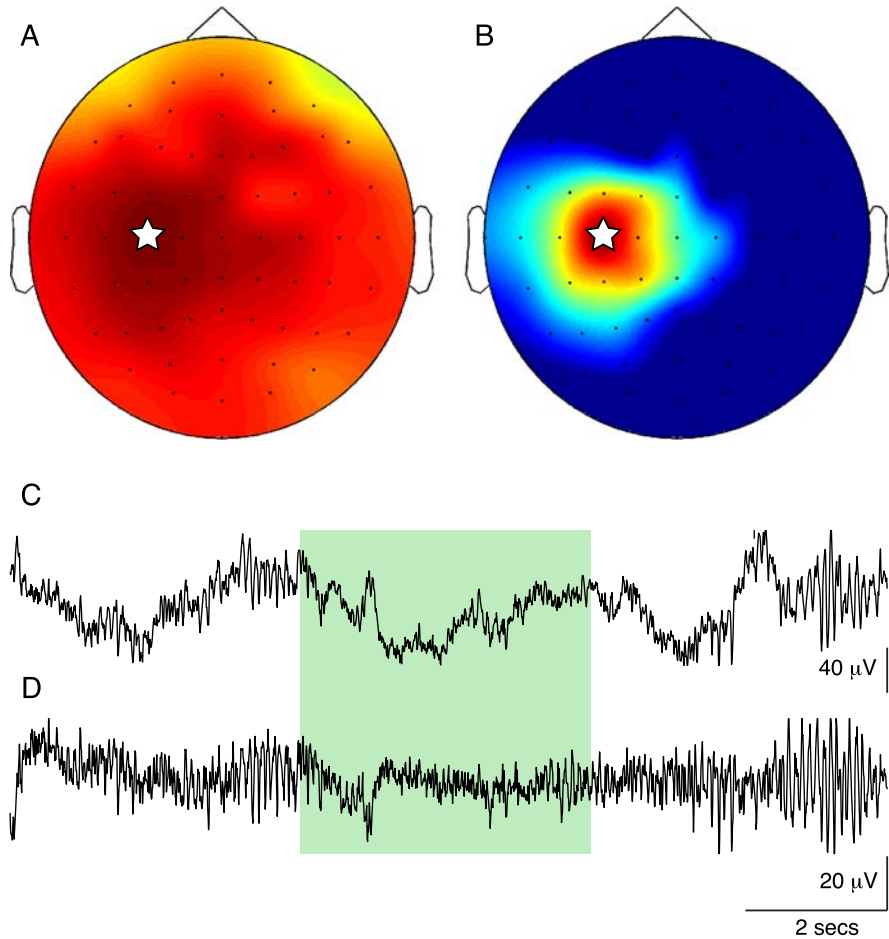   ence (CAR)
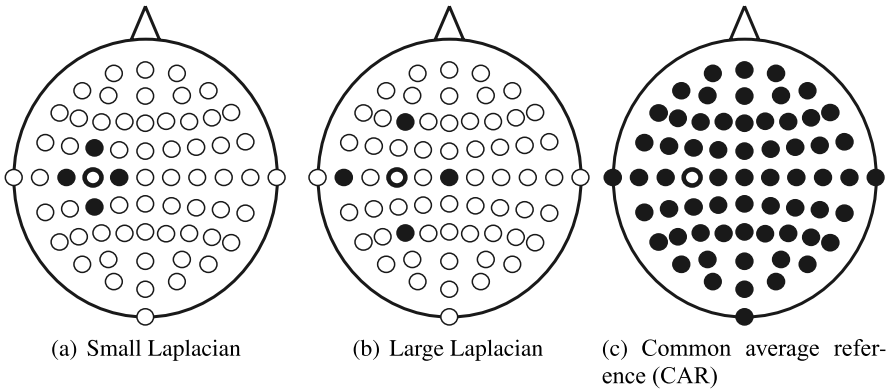
Fig. 2.12 Locations (*filled circles*) involved in different spatial filters applied to location C_3 (see Fig. 2.13) (*open circles*)
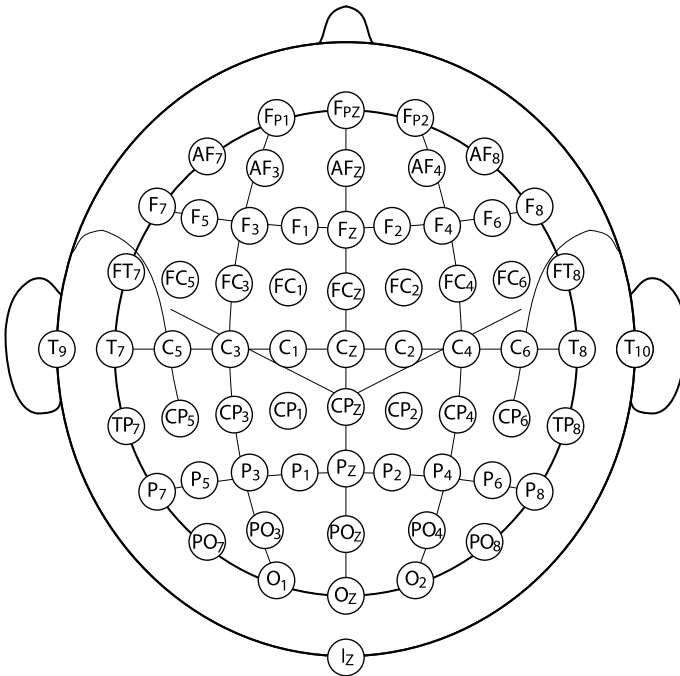
Fig. 2.13 Electrode designations for a 64-channel setup of the extended 10–20 system. (Redrawn from [94])

The Common Average Reference (CAR) filter, another possible spatial high-pass filter, is implemented by re-referencing the potential $s_h(t)$ of each electrode h at each time point t to an estimated reference that is calculated by averaging the signals from all H recorded electrodes (see Eq. 2.3 and Fig. 2.12(c)). In other words, a CAR

Fig. 2.14 Example of application of a Common Average Reference (CAR) spatial filter. Signals are spatially more specific and better highlight beta rhythm suppression during the period indicated by the *green bar* when a CAR filter is applied (**B** and **D**) compared to when it is not (**A** and **C**)

filter calculates the signal amplitude that is common to all electrodes ($\frac{1}{H}\sum_{i=1}^{H} s_i(t)$) and subtracts it from the signal $s_h(t)$ at each location. The CAR and Large Laplacian filters have been shown to provide comparable performance [56].

$$s'_h(t) = s_h(t) - \frac{1}{H}\sum_{i=1}^{H} s_i(t) \qquad (2.3)$$

Whatever the realization of the spatial filter, its main purposes are to deblur the recorded signals so as to derive a more faithful representation of the sources within the brain, and/or to remove the influence of the reference electrode from the signal. The example in Fig. 2.14 illustrates results of this operation on signals recorded

using EEG. In this example, the topographies illustrate the effect of a CAR filter on signals in space: in A, the unfiltered signal is spatially broad, whereas in B, the CAR-filtered signal emphasizes spatially local features. (Color indicates the correlation coefficient r calculated between the signal time course at each location (indicated by small dots) and the signal at the location indicated with the white star.) The signal time courses in C and D (which are recorded at the location marked with a star) illustrate the effect of a CAR filter on beta rhythms that are suppressed by right hand movement. The green bar indicates the period that the subject opened and closed her right hand. Beta rhythm oscillations (around 25 Hz) are suppressed during this period. This effect is more pronounced for the CAR-filtered signal in D compared to the unfiltered data in C. Also, application of the CAR filter removes the slow signal fluctuations seen in C. Thus, this example illustrates that the CAR filter removes some of the signal variance that is not related to the hand movement task.

The second and final step of feature extraction is the application of a temporal filter. Its purpose is to project the input signal in a representation (i.e., domain) in which the brain signals that can be modulated by the user are best expressed. The P300 potential is usually extracted in the time domain simply by averaging the brain responses to the different stimuli. Because mu/beta rhythms represent oscillatory activity, they are usually extracted in the frequency domain as described below.

2.4.3 Feature Extraction: Sensorimotor Rhythms

As described, imagined movements have been shown to produce changes in the mu (i.e., 8–12 Hz) or beta (i.e., 18–25 Hz) frequency band. Thus, for the processing of mu/beta rhythm (i.e., sensorimotor) signals, the frequency domain is most often used, although a recent paper suggested a matched filter in the time domain [38] that better captured the non-sinusoidal components of the mu rhythm. Several methods for the transformation of time domain into the frequency domain have been proposed, such as the Fast Fourier Transform (FFT), wavelet transform, and procedures based on autoregressive parameters. The requirements of BCI systems offer suggestions about which of these methods to select. BCIs are closed-loop systems that should provide feedback many times per second (e.g., typically, at more than 20 Hz) with a minimal group delay. In general, no method can concurrently achieve high resolution in time and frequency. However, the Maximum Entropy Method (MEM) [53], which is based on autoregressive modeling, has a higher temporal resolution (and thus reduced group delay) at a given frequency resolution compared to the FFT and wavelet transforms [53], and is thus advantageous in the context of BCI systems. Whatever its realization, the temporal filter used for mu/beta rhythms transforms time-domain signals $s'_e(t)$ into frequency-domain features $a_e(n)$.

As an example of its function, Fig. 2.15 illustrates application of the temporal filter to data collected using scalp-recorded EEG while a subject imagined hand movement or rested. CAR-filtered signals at each location were converted into the
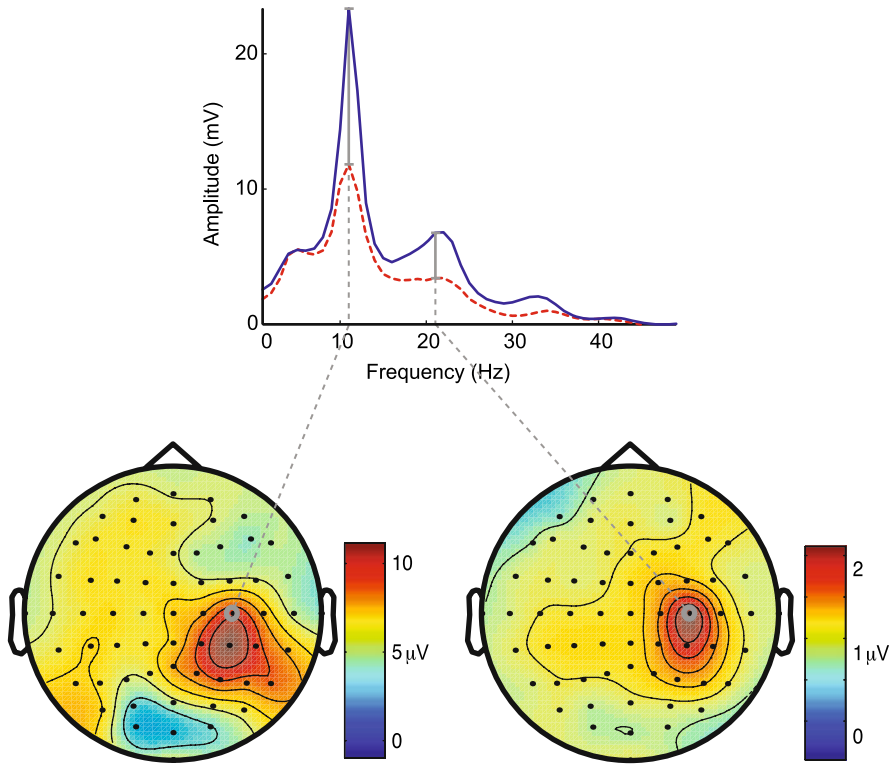
Fig. 2.15 Example analyses of the temporal filter. In this example, EEG was recorded during imagined left hand movement and during rest. The spectrum for rest (*blue solid line*) is different from that for imagined hand movement (*red dashed line*). This difference is sharply focused in frequency (see spectra *above*) and in space (see topographies *below*) and could be used for BCI control

frequency domain using the MEM algorithm and blocks of 400 ms length. The resulting spectra were averaged across blocks. This produced one average spectrum for each location and for each of the two conditions of imagined movement of the left hand and rest. (The example in Fig. 2.15 illustrates spectra at location C4.) The difference in the spectrum between imagined movement (red dashed line) and rest (blue solid line) is evident and is sharply focused in frequency (around 11 and 22 Hz) and space (over location C4 of right sensorimotor cortex). (While in this figure activity at 22 Hz may simply be a harmonic of activity at 11 Hz, evidence suggests that the relationship between mu and beta rhythms may be more complicated [57].) In other words, this particular subject can use particular motor imagery to change the signal amplitude at location C4 and 11/22 Hz and could thus communicate her intent using this particular type of imagery.

To facilitate understanding of the issues in BCI signal processing, the previous sections described the first component of BCI signal processing, feature extraction, which is composed of spatial filtering and temporal filtering. The purpose of feature

extraction is to convert digitized brain signal samples that are recorded at various locations into features (e.g., frequency-domain spectra $a_e(n)$) that express the subject's intent. The second component of BCI signal processing, the translation algorithm, effects this intent by translating these features into device commands. The following section describes a common realization of the translation algorithm.

2.4.4 Translation Algorithm

The second step of BCI signal processing, the translation algorithm, is comprised mainly of a signal translation procedure that converts the set of brain signal features $a_e(n)$ into a set of output signals that control an output device. This translation has been traditionally accomplished using conventional classification/regression procedures. For example, studies have been using linear discriminant analysis [2], neural networks [34, 75], support vector machines [26, 30, 43, 65], and linear regression [54, 55]. To compensate for spontaneous changes in brain signals, the translation algorithm may also include a whitening procedure (e.g., a linear transformation) that produces signals with zero mean and a defined variance such that the output device does not have to account for changes in brain signal characteristics that are not related to the task.

We illustrate the function of a typical approach using an example realization of a translation algorithm using linear regression. Data were derived from the previous example shown in Fig. 2.15. Figure 2.16-A shows the distribution of data samples derived at C4 and 11/22 Hz (i.e., log transformed features $a_1(n)$, $a_2(n)$, respectively). Blue dots show samples that correspond to rest and red dots show samples that correspond to imagined left hand movement. Linear regression determined the coefficients of the linear function that minimized the error between the output of that function ($c(n)$) and arbitrary target values for the two classes (i.e., -1, $+1$). This procedure derived the coefficients of the linear function that could be used to translate the features into an output signal: $c(n) = 2{,}560a_1(n) + 4{,}582a_2(n)$. The histogram of the values of $c(n)$ calculated for the data from the rest class (blue) is different than that calculated for the data from the imagined hand class (red) (see Fig. 2.16-B), which indicates that the user had some level of control over this particular signal. To quantitatively evaluate this level of user control, we determined the value of r^2, i.e., the fraction of the variance in the output signal $c(n)$ that is associated with the classes. We then applied the same linear function to samples from all electrodes. Figure 2.16-C illustrates that, as expected, the signal difference is sharply focused over right sensorimotor cortex.

In summary, BCI signal processing is accomplished using two components. The first component, feature extraction, extracts brain signal features that reflect the user's intent. The second component, the translation algorithm, translates these signal features into output signals that can control an output device. This translation algorithm has traditionally been realized using a variety of classification/regression approaches. In summary, this chapter described relevant principles of BCI operation
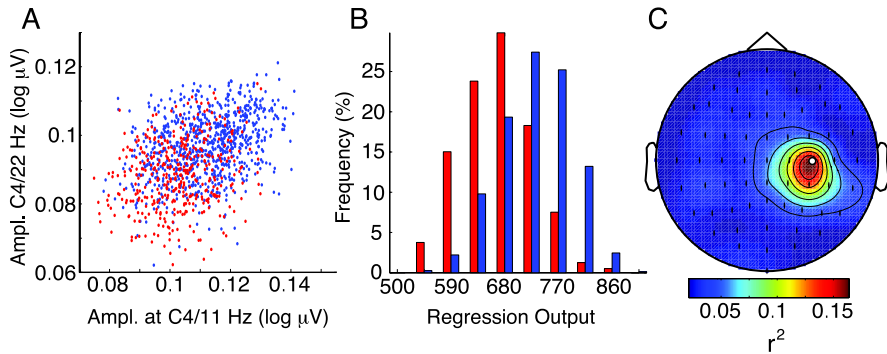
Fig. 2.16 Example of a typical translation algorithm that uses linear regression. **A**: Distribution of signal features (i.e., signal amplitudes at C4 and 11/22 Hz for rest (*blue dots*) and imagined left hand movement (*red dots*)). **B**: Histogram of output values calculated for each of the two classes using linear regression applied to the two features. **C**: As expected, the signal difference is focused over right sensorimotor cortex. See text for details

and associated techniques. The next chapter discusses the general concepts of the BCI2000 platform, and how BCI2000 can implement these techniques.

References

1. Allison, B.Z.: P3 or not P3: toward a better P300 BCI. PhD thesis, University of California, San Diego (2003)
2. Babiloni, F., Cincotti, F., Lazzarini, L., Millan, J., Mourino, J., Varsta, M., Heikkonen, J., Bianchi, L., Marciani, M.G.: Linear classification of low-resolution EEG patterns produced by imagined hand movements. IEEE Trans. Rehabil. Eng. **8**(2), 186–188 (2000)
3. Ball, T., Kern, M., Mutschler, I., Aertsen, A., Schulze-Bonhage, A.: Signal quality of simultaneously recorded invasive and non-invasive EEG. NeuroImage **46**(3), 708–716 (2009). doi:10.1016/j.neuroimage.2009.02.028. http://www.hubmed.org/display.cgi?uids=19264143
4. Bashashati, A., Fatourechi, M., Ward, R.K., Birch, G.E.: A survey of signal processing algorithms in brain–computer interfaces based on electrical brain signals. J. Neural Eng. **4**(2), R32–R57 (2007). doi:10.1088/1741-2560/4/2/R03
5. Bayliss, J.D.: A flexible brain–computer interface. PhD thesis, University of Rochester, Rochester (2001). http://www.cs.rochester.edu/trs/robotics-trs.html
6. Birbaumer, N., Ghanayim, N., Hinterberger, T., Iversen, I., Kotchoubey, B., Kübler, A., Perelmouter, J., Taub, E., Flor, H.: A spelling device for the paralysed. Nature **398**(6725), 297–298 (1999)
7. Bullara, L.A., Agnew, W.F., Yuen, T.G., Jacques, S., Pudenz, R.H.: Evaluation of electrode array material for neural prostheses. Neurosurg. **5**(6), 681–686 (1979)
8. Chatrian, G.E.: The mu rhythm. In: Handbook of Electroencephalography and Clinical Neurophysiology. The EEG of the Waking Adult, pp. 46–69. Elsevier, Amsterdam (1976)
9. Chin, C.M., Popovic, M.R., Thrasher, A., Cameron, T., Lozano, A., Chen, R.: Identification of arm movements using correlation of electrocorticographic spectral components and kinematic recordings. J. Neural Eng. **4**(2), 146–158 (2007). doi:10.1088/1741-2560/4/2/014
10. Coyle, S., Ward, T., Markham, C., McDarby, G.: On the suitability of near-infrared (NIR) systems for next-generation brain–computer interfaces. Physiol. Meas. **25**(4), 815–822 (2004)

11. Coyle, S.M., Ward, T.E., Markham, C.M.: Brain–computer interface using a simplified functional near-infrared spectroscopy system. J. Neural Eng. **4**(3), 219–226 (2007). doi:10.1088/1741-2560/4/3/007
12. Crone, N.E., Miglioretti, D.L., Gordon, B., Sieracki, J.M., Wilson, M.T., Uematsu, S., Lesser, R.P.: Functional mapping of human sensorimotor cortex with electrocorticographic spectral analysis. i. Alpha and beta event-related desynchronization. Brain **121** (12), 2271–2299 (1998)
13. Crone, N.E., Miglioretti, D.L., Gordon, B., Lesser, R.P.: Functional mapping of human sensorimotor cortex with electrocorticographic spectral analysis. ii. Event-related synchronization in the gamma band. Brain **121** (12), 2301–2315 (1998)
14. Crone, N.E., Hao, L., Hart, J., Boatman, D., Lesser, R.P., Irizarry, R., Gordon, B.: Electrocorticographic gamma activity during word production in spoken and sign language. Neurol. **57**(11), 2045–2053 (2001)
15. Donchin, E.: Presidential address, 1980. Surprise!...Surprise? Psychophysiol. **18**(5), 493–513 (1981)
16. Donchin, E., Coles, M.: Is the P300 component a manifestation of context updating? Behav. Brain Sci. **11**(3), 357–427 (1988)
17. Donchin, E., Smith, D.B.: The contingent negative variation and the late positive wave of the average evoked potential. Electroencephalogr. Clin. Neurophysiol. **29**(2), 201–203 (1970)
18. Donchin, E., Heffley, E., Hillyard, S.A., Loveless, N., Maltzman, I., Ohman, A., Rösler, F., Ruchkin, D., Siddle, D.: Cognition and event-related potentials. ii. The orienting reflex and P300. Ann. N.Y. Acad. Sci. **425**, 39–57 (1984)
19. Donchin, E., Spencer, K.M., Wijesinghe, R.: The mental prosthesis: assessing the speed of a P300-based brain–computer interface. IEEE Trans. Rehabil. Eng. **8**(2), 174–179 (2000)
20. Donoghue, J., Nurmikko, A., Friehs, G., Black, M.: Development of neuromotor prostheses for humans. Suppl. Clin. Neurophysiol. **57**, 592–606 (2004)
21. Donoghue, J.P., Nurmikko, A., Black, M., Hochberg, L.R.: Assistive technology and robotic control using motor cortex ensemble-based neural interface systems in humans with tetraplegia. J. Physiol. **579**(3), 603–611 (2007). doi:10.1113/jphysiol.2006.127209
22. Farwell, L.A., Donchin, E.: Talking off the top of your head: toward a mental prosthesis utilizing event-related brain potentials. Electroencephalogr. Clin. Neurophysiol. **70**(6), 510–523 (1988)
23. Felton, E.A., Wilson, J.A., Williams, J.C., Garell, P.C.: Electrocorticographically controlled brain–computer interfaces using motor and sensory imagery in patients with temporary subdural electrode implants. Report of four cases. J. Neurosurg. **106**(3), 495–500 (2007)
24. Fisch, B.J.: Spehlmann's EEG Primer, 2nd edn. Elsevier, Amsterdam (1991)
25. Freeman, W.J., Holmes, M.D., Burke, B.C., Vanhatalo, S.: Spatial spectra of scalp EEG and EMG from awake humans. Clin. Neurophysiol. **114**, 1053–1068 (2003)
26. Garrett, D., Peterson, D.A., Anderson, C.W., Thaut, M.H.: Comparison of linear, nonlinear, and feature selection methods for EEG signal classification. IEEE Trans. Rehabil. Eng. **11**(2), 141–144 (2003)
27. Gastaut, H.: Etude electrocorticographique de la reactivite des rythmes rolandiques. Rev. Neurol. **87**, 176–182 (1952)
28. Graimann, B., Huggins, J.E., Schlögl, A., Levine, S.P., Pfurtscheller, G.: Detection of movement-related desynchronization patterns in ongoing single-channel electrocorticogram. IEEE Trans. Neural Syst. Rehabil. Eng. **11**(3), 276–281 (2003)
29. Guger, C., Ramoser, H., Pfurtscheller, G.: Real-time EEG analysis with subject-specific spatial patterns for a brain–computer interface (BCI). IEEE Trans. Rehabil. Eng. **8**(4), 447–456 (2000)
30. Gysels, E., Renevey, P., Celka, P.: SVM-based recursive feature elimination to compare phase synchronization computed from broadband and narrowband EEG signals in brain–computer interfaces. Signal Process. **85**(11), 2178–2189 (2005)
31. Hjorth, B.: Principles for transformation of scalp EEG from potential field into source distribution. J. Clin. Neurophysiol. **8**(4), 391–396 (1991)

32. Hochberg, L.R., Serruya, M.D., Friehs, G.M., Mukand, J.A., Saleh, M., Caplan, A.H., Branner, A., Chen, D., Penn, R.D., Donoghue, J.P.: Neuronal ensemble control of prosthetic devices by a human with tetraplegia. Nature **442**(7099), 164–171 (2006). doi:10.1038/nature04970

33. Hoffmann, U., Vesin, J.M., Ebrahimi, T., Diserens, K.: An efficient P300-based brain–computer interface for disabled subjects. J. Neurosci. Methods **167**(1), 115–125 (2008). doi:10.1016/j.jneumeth.2007.03.005

34. Huan, N.J., Palaniappan, R.: Neural network classification of autoregressive features from electroencephalogram signals for brain–computer interface design. J. Neural Eng. **1**(3), 142–150 (2004)

35. Jasper, H.H.: The ten twenty electrode system of the international federation. Electroencephalogr. Clin. Neurophysiol. **10**, 371–375 (1958)

36. Kostov, A., Polak, M.: Parallel man–machine training in development of EEG-based cursor control. IEEE Trans. Rehabil. Eng. **8**(2), 203–205 (2000)

37. Kozelka, J.W., Pedley, T.A.: Beta and mu rhythms. J. Clin. Neurophysiol. **7**, 191–207 (1990)

38. Krusienski, D.J., Schalk, G., McFarland, D.J., Wolpaw, J.R.: A mu-rhythm matched filter for continuous control of a brain–computer interface. IEEE Trans. Biomed. Eng. **54**(2), 273–280 (2007). doi:10.1109/TBME.2006.886661

39. Kübler, A., Kotchoubey, B., Hinterberger, T., Ghanayim, N., Perelmouter, J., Schauer, M., Fritsch, C., Taub, E., Birbaumer, N.: The Thought Translation Device: a neurophysiological approach to communication in total motor paralysis. Exp. Brain Res. **124**(2), 223–232 (1999)

40. Kübler, A., Nijboer, F., Mellinger, J., Vaughan, T.M., Pawelzik, H., Schalk, G., McFarland, D.J., Birbaumer, N., Wolpaw, J.R.: Patients with ALS can use sensorimotor rhythms to operate a brain–computer interface. Neurol. **64**(10), 1775–1777 (2005). doi:10.1212/01.WNL.0000158616.43002.6D

41. Lachaux, J.P., Fonlupt, P., Kahane, P., Minotti, L., Hoffmann, D., Bertrand, O., Baciu, M.: Relationship between task-related gamma oscillations and bold signal: new insights from combined fMRI and intracranial EEG. Hum. Brain Mapp. **28**(12), 1368–1375 (2007). doi:10.1002/hbm.20352

42. LaConte, S.M., Peltier, S.J., Hu, X.P.: Real-time fMRI using brain-state classification. Hum. Brain Mapp. **28**(10), 1033–1044 (2007). doi:10.1002/hbm.20326. http://www.hubmed.org/display.cgi?uids=17133383

43. Lal, T.N., Schroder, M., Hinterberger, T., Weston, J., Bogdan, M., Birbaumer, N., Schölkopf, B.: Support vector channel selection in BCI. IEEE Trans. Biomed. Eng. **51**(6), 1003–1010 (2004)

44. Le, J., Gevins, A.: Method to reduce blur distortion from EEG's using a realistic head model. IEEE Trans. Biomed. Eng. **40**(6), 517–528 (1993)

45. Lebedev, M.A., Carmena, J.M., O'Doherty, J.E., Zacksenhouse, M., Henriquez, C.S., Principe, J.C., Nicolelis, M.A.: Cortical ensemble adaptation to represent velocity of an artificial actuator controlled by a brain–machine interface. J. Neurosci. **25**(19), 4681–4693 (2005). doi:10.1523/JNEUROSCI.4088-04.2005

46. Leuthardt, E., Schalk, G., JR, J.W., Ojemann, J., Moran, D.: A brain–computer interface using electrocorticographic signals in humans. J. Neural Eng. **1**(2), 63–71 (2004)

47. Leuthardt, E., Miller, K., Schalk, G., Rao, R., Ojemann, J.: Electrocorticography-based brain computer interface – the Seattle experience. IEEE Trans. Neural Syst. Rehabil. Eng. **14**, 194–198 (2006)

48. Leuthardt, E., Miller, K., Anderson, N., Schalk, G., Dowling, J., Miller, J., Moran, D., Ojemann, J.: Electrocorticographic frequency alteration mapping: a clinical technique for mapping the motor cortex. Neurosurg. **60**, 260–270, discussion 270–271 (2007). doi:10.1227/01.NEU.0000255413.70807.6E

49. Loeb, G.E., Walker, A.E., Uematsu, S., Konigsmark, B.W.: Histological reaction to various conductive and dielectric films chronically implanted in the subdural space. J. Biomed. Mater. Res. **11**(2), 195–210 (1977). doi:10.1002/jbm.820110206

50. Lotte, F., Congedo, M., Lécuyer, A., Lamarche, F., Arnaldi, B.: A review of classification algorithms for EEG-based brain–computer interfaces. J. Neural Eng. **4**(2), 1–1 (2007). doi:10.1088/1741-2560/4/2/R01

51. Makeig, S., Jung, T., Bell, A., Sejnowski, T.: Independent component analysis of electroencephalographic data. In: Advances in Neural Information Processing Systems, vol. 8, pp. 145–151. MIT Press, Cambridge (1996)

52. Margalit, E., Weiland, J., Clatterbuck, R., Fujii, G., Maia, M., Tameesh, M., Torres, G., D'Anna, S., Desai, S., Piyathaisere, D., Olivi, A., de Juan, E.J., Humayun, M.: Visual and electrical evoked response recorded from subdural electrodes implanted above the visual cortex in normal dogs under two methods of anesthesia. J. Neurosci. Methods **123**(2), 129–137 (2003)

53. Marple, S.L.: Digital Spectral Analysis: With Applications. Prentice–Hall, Englewood Cliffs (1987)

54. McFarland, D.J., Neat, G.W., Wolpaw, J.R.: An EEG-based method for graded cursor control. Psychobiol. **21**, 77–81 (1993)

55. McFarland, D.J., Lefkowicz, T., Wolpaw, J.R.: Design and operation of an EEG-based brain–computer interface (BCI) with digital signal processing technology. Behav. Res. Methods Instrum. Comput. **29**, 337–345 (1997)

56. McFarland, D.J., McCane, L.M., David, S.V., Wolpaw, J.R.: Spatial filter selection for EEG-based communication. Electroencephalogr. Clin. Neurophysiol. **103**(3), 386–394 (1997)

57. McFarland, D.J., Miner, L.A., Vaughan, T.M., Wolpaw, J.R.: Mu and beta rhythm topographies during motor imagery and actual movements. Brain Topogr. **12**(3), 177–186 (2000)

58. McFarland, D., Anderson, C.W., Müller, K.R., Schlögl, A., Krusienski, D.J.: BCI meeting 2005 – workshop on BCI signal processing: feature extraction and translation. IEEE Trans. Neural Syst. Rehabil. Eng. **14**(2), 135–138 (2006)

59. McFarland, D.J., Krusienski, D.J., Sarnacki, W.A., Wolpaw, J.R.: Emulation of computer mouse control with a noninvasive brain–computer interface. J. Neural Eng. **5**(2), 101–110 (2008). doi:10.1088/1741-2560/5/2/001. http://www.hubmed.org/display.cgi?uids=18367779

60. Mellinger, J., Schalk, G., Braun, C., Preissl, H., Rosenstiel, W., Birbaumer, N., Kübler, A.: An MEG-based brain–computer interface (BCI). NeuroImage **36**(3), 581–593 (2007). doi:10.1016/j.neuroimage.2007.03.019

61. Millán, J. del R., Renkens, F., Mouriño, J., Gerstner, W.: Noninvasive brain-actuated control of a mobile robot by human EEG. IEEE Trans. Biomed. Eng. **51**(6), 1026–1033 (2004)

62. Miller, K., Leuthardt, E., Schalk, G., Rao, R., Anderson, N., Moran, D., Miller, J., Ojemann, J.: Spectral changes in cortical surface potentials during motor movement. J. Neurosci. **27**, 2424–2432 (2007). doi:10.1523/JNEUROSCI.3886-06.2007. http://www.jneurosci.org/cgi/content/abstract/27/9/2424

63. Morgan, S.T., Hansen, J.C., Hillyard, S.A.: Selective attention to stimulus location modulates the steady-state visual evoked potential. Proc. Natl. Acad. Sci. USA **93**(10), 4770–4774 (1996)

64. Müller, K., Blankertz, B.: Toward noninvasive brain–computer interfaces. IEEE Signal Process. Mag. **23**(5), 126–128 (2006)

65. Müller, K.R., Anderson, C.W., Birch, G.E.: Linear and nonlinear methods for brain–computer interfaces. IEEE Trans. Rehabil. Eng. **11**(2), 165–169 (2003)

66. Müller, K.R., Tangermann, M., Dornhege, G., Krauledat, M., Curio, G., Blankertz, B.: Machine learning for real-time single-trial EEG-analysis: from brain–computer interfacing to mental state monitoring. J. Neurosci. Methods **167**(1), 82–90 (2008). doi:10.1016/j.jneumeth.2007.09.022. http://www.hubmed.org/display.cgi?uids=18031824

67. Musallam, S., Corneil, B.D., Greger, B., Scherberger, H., Andersen, R.A.: Cognitive control signals for neural prosthetics. Science **305**(5681), 258–262 (2004). doi:10.1126/science.1097938

68. Neshige, R., Murayama, N., Tanoue, K., Kurokawa, H., Igasaki, T.: Optimal methods of stimulus presentation and frequency analysis in P300-based brain–computer interfaces for patients with severe motor impairment. Suppl. Clin. Neurophysiol. **59**, 35–42 (2006)

69. Niedermeyer, E.: The normal EEG of the waking adult. In: Niedermeyer, E., Lopes da Silva, F.H. (eds.) Electroencephalography: Basic Principles, Clinical Applications and Related Fields, 4th edn., pp. 149–173. Williams and Wilkins, Baltimore (1999)

70. Pfurtscheller, G.: EEG event-related desynchronization (ERD) and event-related synchronization (ERS). In: Niedermeyer, E., Lopes da Silva, F.H. (eds.) Electroencephalography: Basic Principles, Clinical Applications and Related Fields, 4th edn., pp. 958–967. Williams and Wilkins, Baltimore (1999)

71. Pfurtscheller, G., Berghold, A.: Patterns of cortical activation during planning of voluntary movement. Electroencephalogr. Clin. Neurophysiol. **72**, 250–258 (1989)

72. Pfurtscheller, G., Neuper, C.: Motor imagery activates primary sensorimotor area in humans. Neurosci. Lett. **239**, 65–68 (1997)

73. Pfurtscheller, G., Flotzinger, D., Kalcher, J.: Brain–computer interface – a new communication device for handicapped persons. J. Microcomput. Appl. **16**, 293–299 (1993)

74. Pfurtscheller, G., Neuper, C., Kalcher, J.: 40-Hz oscillations during motor behavior in man. Neurosci. Lett. **164**(1–2), 179–182 (1993)

75. Pfurtscheller, G., Neuper, C., Flotzinger, D., Pregenzer, M.: EEG-based discrimination between imagination of right and left hand movement. Electroencephalogr. Clin. Neurophysiol. **103**(6), 642–651 (1997)

76. Pfurtscheller, G., Guger, C., Müller, G., Krausz, G., Neuper, C.: Brain oscillations control hand orthosis in a tetraplegic. Neurosci. Lett. **292**(3), 211–214 (2000)

77. Pfurtscheller, G., Graimann, B., Huggins, J.E., Levine, S.P., Schuh, L.A.: Spatiotemporal patterns of beta desynchronization and gamma synchronization in corticographic data during self-paced movement. Clin. Neurophysiol. **114**(7), 1226–1236 (2003)

78. Piccione, F., Giorgi, F., Tonin, P., Priftis, K., Giove, S., Silvoni, S., Palmas, G., Beverina, F.: P300-based brain computer interface: reliability and performance in healthy and paralysed participants. Clin. Neurophysiol. **117**(3), 531–537 (2006). doi:10.1016/j.clinph.2005.07.024

79. Pistohl, T., Ball, T., Schulze-Bonhage, A., Aertsen, A., Mehring, C.: Prediction of arm movement trajectories from ECoG-recordings in humans. J. Neurosci. Methods **167**(1), 105–114 (2008)

80. Pritchard, W.S.: Psychophysiology of P300. Psychol. Bull. **89**(3), 506–540 (1981)

81. Ramoser, H., Müller-Gerking, J., Pfurtscheller, G.: Optimal spatial filtering of single trial EEG during imagined hand movement. IEEE Trans. Rehabil. Eng. **8**(4), 441–446 (2000)

82. Ramsey, N.F., van de Heuvel, M.P., Kho, K.H., Leijten, F.S.: Towards human BCI applications based on cognitive brain systems: an investigation of neural signals recorded from the dorsolateral prefrontal cortex. IEEE Trans. Neural Syst. Rehabil. Eng. **14**(2), 214–217 (2006). http://www.hubmed.org/display.cgi?uids=16792297

83. Sanchez, J.C., Gunduz, A., Carney, P.R., Principe, J.C.: Extraction and localization of mesoscopic motor control signals for human ECoG neuroprosthetics. J. Neurosci. Methods **167**(1), 63–81 (2008). doi:10.1016/j.jneumeth.2007.04.019

84. Santhanam, G., Ryu, S.I., Yu, B.M., Afshar, A., Shenoy, K.V.: A high-performance brain–computer interface. Nature **442**(7099), 195–198 (2006). doi:10.1038/nature04968

85. Schalk, G., McFarland, D., Hinterberger, T., Birbaumer, N., Wolpaw, J.: BCI2000: a general-purpose brain–computer interface (BCI) system. IEEE Trans. Biomed. Eng. **51**, 1034–1043 (2004)

86. Schalk, G., Kubánek, J., Miller, K.J., Anderson, N.R., Leuthardt, E.C., Ojemann, J.G., Limbrick, D., Moran, D., Gerhardt, L.A., Wolpaw, J.R.: Decoding two-dimensional movement trajectories using electrocorticographic signals in humans. J. Neural Eng. **4**(3), 264–275 (2007). doi:10.1088/1741-2560/4/3/012

87. Schalk, G., Miller, K.J., Anderson, N.R., Wilson, J.A., Smyth, M.D., Ojemann, J.G., Moran, D.W., Wolpaw, J.R., Leuthardt, E.C.: Two-dimensional movement control using electrocorticographic signals in humans. J. Neural Eng. **5**(1), 75–84 (2008). doi:10.1088/1741-2560/5/1/008

88. Sellers, E.W., Donchin, E.: A P300-based brain–computer interface: initial tests by ALS patients. Clin. Neurophysiol. **117**(3), 538–548 (2006). doi:10.1016/j.clinph.2005.06.027

89. Sellers, E.W., Kübler, A., Donchin, E.: Brain–computer interface research at the University of South Florida Cognitive Psychophysiology Laboratory: the P300 Speller. IEEE Trans. Neural Syst. Rehabil. Eng. **14**(2), 221–224 (2006)

90. Sellers, E.W., Krusienski, D.J., McFarland, D.J., Vaughan, T.M., Wolpaw, J.R.: A P300 event-related potential brain–computer interface (BCI): the effects of matrix size and inter stimulus interval on performance. Biol. Psychol. **73**(3), 242–252 (2006). doi:10.1016/j.biopsycho.2006.04.007

91. Serby, H., Yom-Tov, E., Inbar, G.F.: An improved P300-based brain–computer interface. IEEE Trans. Neural Syst. Rehabil. Eng. **13**(1), 89–98 (2005)

92. Serruya, M., Hatsopoulos, N., Paninski, L., Fellows, M., Donoghue, J.: Instant neural control of a movement signal. Nature **416**(6877), 141–142 (2002)

93. Shain, W., Spataro, L., Dilgen, J., Haverstick, K., Retterer, S., Isaacson, M., Saltzman, M., Turner, J.: Controlling cellular reactive responses around neural prosthetic devices using peripheral and local intervention strategies. IEEE Trans. Neural Syst. Rehabil. Eng. **11**, 186–188 (2003)

94. Sharbrough, F., Chatrian, G., Lesser, R., Luders, H., Nuwer, M., Picton, T.: American electroencephalographic society guidelines for standard electrode position nomenclature. Electroencephalogr. Clin. Neurophysiol. **8**, 200–202 (1991)

95. Shenoy, K., Meeker, D., Cao, S., Kureshi, S., Pesaran, B., Buneo, C., Batista, A., Mitra, P., Burdick, J., Andersen, R.: Neural prosthetic control signals from plan activity. Neurorep. **14**(4), 591–596 (2003)

96. Sinai, A., Bowers, C.W., Crainiceanu, C.M., Boatman, D., Gordon, B., Lesser, R.P., Lenz, F.A., Crone, N.E.: Electrocorticographic high gamma activity versus electrical cortical stimulation mapping of naming. Brain **128**(7), 1556–1570 (2005). doi:10.1093/brain/awh491

97. Sitaram, R., Caria, A., Birbaumer, N.: Hemodynamic brain–computer interfaces for communication and rehabilitation. Neural Netw. **22**(9), 1320–1328 (2009). doi:10.1016/j.neunet.2009.05.009. http://www.hubmed.org/display.cgi?uids=19524399

98. Sitaram, R., Caria, A. Veit, R., Gaber, T., Rota, G., Kübler, A., Birbaumer, N.: fMRI brain–computer interface: a tool for neuroscientific research and treatment. Comput. Intell. Neurosci. **2007**, Article ID 25487 (10 pages) (2007). doi:10.1155/2007/25487

99. Staba, R.J., Wilson, C.L., Bragin, A., Fried, I., Engel, J.: Quantitative analysis of high-frequency oscillations (80–500 Hz) recorded in human epileptic hippocampus and entorhinal cortex. J. Neurophysiol. **88**(4), 1743–1752 (2002)

100. Stice, P., Muthuswamy, J.: Assessment of gliosis around moveable implants in the brain. J. Neural Eng. **6**(4), 046004 (2009). doi:10.1088/1741-2560/6/4/046004

101. Sutter, E.E.: The brain response interface: communication through visually guided electrical brain responses. J. Microcomput. Appl. **15**, 31–45 (1992)

102. Sutton, S., Braren, M., Zubin, J., John, E.R.: Evoked-potential correlates of stimulus uncertainty. Science **150**(700), 1187–1188 (1965)

103. Taylor, D.M., Tillery, S.I., Schwartz, A.B.: Direct cortical control of 3D neuroprosthetic devices. Science **296**, 1829–1832 (2002)

104. Toro, C., Cox, C., Friehs, G., Ojakangas, C., Maxwell, R., Gates, J.R., Gumnit, R.J., Ebner, T.J.: 8–12 Hz rhythmic oscillations in human motor cortex during two-dimensional arm movements: evidence for representation of kinematic parameters. Electroencephalogr. Clin. Neurophysiol. **93**(5), 390–403 (1994)

105. Turner, J.N., Ancin, H., Becker, D., Szarowski, D.H., Holmes, M., O'Connor, N., Wang, M., Holmes, T.J., Roysam, B.: Automated image analysis technologies for biological 3-d light microscopy. Int. J. Imaging Syst. Technol., Spec. Issue Microsc. **8**, 240–254 (1997)

106. Vaughan, T.M., McFarland, D.J., Schalk, G., Sarnacki, W.A., Krusienski, D.J., Sellers, E.W., Wolpaw, J.R.: The Wadsworth BCI research and development program: at home with BCI. IEEE Trans. Neural Syst. Rehabil. Eng. **14**(2), 229–233 (2006)

107. Walter, W.G., Cooper, R., Aldridge, V.J., McCallum, W.C., Winter, A.L.: Contingent negative variation: an electric sign of sensorimotor association and expectancy in the human brain. Nature **203**, 380–384 (1964)

108. Weiskopf, N., Veit, R., Erb, M., Mathiak, K., Grodd, W., Goebel, R., Birbaumer, N.: Physiological self-regulation of regional brain activity using real-time functional magnetic resonance imaging (fMRI): methodology and exemplary data. NeuroImage **19**(3), 577–586 (2003)

109. Weiskopf, N., Mathiak, K., Bock, S.W., Scharnowski, F., Veit, R., Grodd, W., Goebel, R., Birbaumer, N.: Principles of a brain–computer interface (BCI) based on real-time functional magnetic resonance imaging (fMRI). IEEE Trans. Biomed. Eng. **51**(6), 966–970 (2004)

110. Weiskopf, N., Scharnowski, F., Veit, R., Goebel, R., Birbaumer, N., Mathiak, K.: Self-regulation of local brain activity using real-time functional magnetic resonance imaging (fMRI). J. Physiol. Paris **98**(4–6), 357–373 (2004). doi:10.1016/j.jphysparis.2005.09.019

111. Wilson, J., Felton, E., Garell, P., Schalk, G., Williams, J.: ECoG factors underlying multimodal control of a brain–computer interface. IEEE Trans. Neural Syst. Rehabil. Eng. **14**, 246–250 (2006)

112. Wolpaw, J., Birbaumer, N.: Brain–computer interfaces for communication and control. In: Selzer, M., Clarke, S., Cohen, L., Duncan, P., Gage, F. (eds.) Textbook of Neural Repair and Rehabilitation; Neural Repair and Plasticity, pp. 602–614. Cambridge University Press, Cambridge (2006)

113. Wolpaw, J.R., McFarland, D.J.: Multichannel EEG-based brain–computer communication. Electroencephalogr. Clin. Neurophysiol. **90**(6), 444–449 (1994)

114. Wolpaw, J.R., McFarland, D.J.: Control of a two-dimensional movement signal by a noninvasive brain–computer interface in humans. Proc. Natl. Acad. Sci. USA **101**(51), 17849–17854 (2004). doi:10.1073/pnas.0403504101. http://www.hubmed.org/display.cgi?uids=15585584

115. Wolpaw, J., McFarland, D., Cacace, A.: Preliminary studies for a direct brain-to-computer parallel interface. In: Projects for Persons with Disabilities. IBM Technical Symposium, pp. 11–20 (1986)

116. Wolpaw, J.R., McFarland, D.J., Neat, G.W., Forneris, C.A.: An EEG-based brain–computer interface for cursor control. Electroencephalogr. Clin. Neurophysiol. **78**(3), 252–259 (1991)

117. Wolpaw, J.R., Birbaumer, N., McFarland, D.J., Pfurtscheller, G., Vaughan, T.M.: Brain–computer interfaces for communication and control. Electroencephalogr. Clin. Neurophysiol. **113**(6), 767–791 (2002)

118. Yoo, S.S., Fairneny, T., Chen, N.K., Choo, S.E., Panych, L.P., Park, H., Lee, S.Y., Jolesz, F.A.: Brain–computer interface using fMRI: spatial navigation by thoughts. Neurorep. **15**(10), 1591–1595 (2004)

119. Yuen, T.G., Agnew, W.F., Bullara, L.A.: Tissue response to potential neuroprosthetic materials implanted subdurally. Biomaterials **8**(2), 138–141 (1987)